Mal3, the Fission Yeast Homologue of the Human APC-interacting Protein EB-1 Is Required for Microtubule Integrity and the Maintenance of Cell Form

Jens D. Beinhauer,* Iain M. Hagan,‡ Johannes H. Hegemann,* and Ursula Fleig*

*Institut für Mikrobiologie und Molekularbiologie, Justus-Liebig-Universität Giessen, 35392 Giessen, Germany and ‡School of Biological Sciences, The University of Manchester, M13 9PT, United Kingdom

Abstract. Through a screen designed to isolate novel fission yeast genes required for chromosome segregation, we have identified *mal3[+]*. The *mal3-1* mutation decreased the transmission fidelity of a nonessential minichromosome and altered sensitivity to microtubule-destabilizing drugs. Sequence analysis revealed that the 35-kD Mal3 is a member of an evolutionary conserved protein family. Its human counterpart EB-1 was identified in an interaction screen with the tumour suppressor protein APC. EB-1 was able to substitute for the complete loss of the *mal3[+]* gene product suggesting that the two proteins might have similar functions. Cells containing a *mal3* null allele were viable but showed a variety of phenotypes, including impaired control of cell shape. A fusion protein of Mal3 with the *Aequorea victoria* green fluorescent protein led to in vivo visualization of both cytoplasmic and mitotic microtubule structures indicating association of Mal3 with microtubules. The absence of Mal3 protein led to abnormally short, often faint cytoplasmic microtubules as seen by indirect antitubulin immunofluorescence. While loss of the *mal3[+]* gene product had no gross effect on mitotic spindle morphology, overexpression of *mal3[+]* compromised spindle formation and function and led to severe growth inhibition and abnormal cell morphology. We propose that Mal3 plays a role in regulating the integrity of microtubules possibly by influencing their stability.

PRECISE duplication of the genetic material and its subsequent accurate segregation into two daughter cells are essential properties of the eucaryotic cell cycle, that ensure the faithful inheritance of genetic information. Genomic stability is vital for the survival of an organism and genetic instability has long been considered an integral characteristic of certain types of cancers (reviewed in Hartwell, 1992).

Entry into mitosis is controlled by the activation of the protein kinase complex MPF which results in chromosome condensation and the formation of the mitotic spindle. The spindle is a dynamic array of microtubules and a large number of microtubule-associated proteins (Hoyt and Geiser, 1996; reviewed in Hyman and Karsenti, 1996; Walczak and Mitchison, 1996). Alignment of chromosomes to the middle of the spindle in metaphase and the subsequent separation of the sister chromatids to opposite poles in anaphase (reviewed in Yanagida, 1995) requires interactions between kinetochores and spindle microtubules. Although substantial progress has been made in recent years in identifying components required for spindle function, such as mitotic motor proteins (Hoyt and Geiser, 1996), the complexity of the system suggests that a large number of molecules involved in ensuring the accurate segregation of the chromosomes await identification.

Mutations in genes required for chromosome transmission fidelity can be identified by scoring for the increased loss of a genetically marked, nonessential minichromosome. Using such an assay we have identified a number of new factors required for chromosome segregation (Fleig et al., 1996). Here we report the characterization of a further component *mal3[+]*. Cloning of the wild-type *mal3[+]* gene revealed that the 35-kD predicted product of the *mal3[+]* gene, Mal3, belongs to an evolutionary conserved protein family. A human homologue of Mal3 is EB-1, which was identified on the basis of its ability to interact with the carboxyl terminus of the tumour-suppressor protein adenomatous polyposis coli (APC)[1] (Su et al., 1995).

Germline mutations in the APC gene lead to the inherited disease familial adenomatous polyposis (FAP). FAP

---

1. *Abbreviations used in this paper*: APC, adenomatous polyposis coli; FAP, familial adenomatous polyposis; GFP, green fluorescent protein; ORF, open reading frame; MAP, microtubule-associating protein; TBZ, thiabendazole.

shows a dominant mode of inheritance occurring in 1 in 7,000 individuals and results in the development of hundreds to thousands of colorectal tumors in early adult life. Some of these will give rise to carcinomas (reviewed in Kinzler and Vogelstein, 1996). APC gene defects are also present in the majority of sporadic colorectal tumors and represent an early event in colorectal tumor development (Groden et al., 1991; Nishisho et al., 1991). The APC gene encodes a 310-kD cytoplasmic protein with no strong homologies to proteins of known function (reviewed in Kinzler and Vogelstein, 1996). APC has been implicated in a number of cellular processes including the regulation of directed cell migration (reviewed in Polakis, 1995; Näthke et al., 1996; Wong et al., 1996). The amino-terminal part of APC contains an oligomerization domain, while the central third mediates β-catenin binding (reviewed in Kinzler and Vogelstein, 1996; Pfeifer, 1996). Association of APC with β-catenin links APC to the process of cell adhesion as well as placing it into the Drosophila Wg/ mouse Wnt signal transduction pathway (reviewed in Kemler, 1993; Kinzler and Vogelstein, 1996; Pfeifer, 1996). The carboxyl-terminal end of APC is required for association with EB-1, the human homologue of the Drosophila tumor suppressor protein DLG and the microtubule cytoskeleton (Munemitsu et al., 1994; Smith et al., 1994; Matsumine et al., 1996). Over 95% of APC mutations in FAP and sporadic tumors result in truncations which delete the carboxyl-terminal third of the protein (reviewed in Polakis, 1995) suggesting that interactions in this region of APC play key roles in regulating the growth-controlling function of APC.

Here we show by the ability of EB-1 to substitute for fission yeast Mal3 function that the two proteins appear to have similar functions, implying that an analysis of fission yeast Mal3 could provide valuable insight into the function of the APC-interacting protein EB-1. Our data indicate that the microtubule-interacting *mal3+* gene product plays an important role in regulating/maintaining the integrity of microtubule arrays.

Materials and Methods

Media and Strains

The *Schizosaccharomyces pombe* strains HM348 (*h+*, *leu1-32, fur1, ade6-M210, tps1,* Ch[16] [*ade6-M216*]) (Niwa et al., 1986), YP10.22 (*h−*, *leu1-32, ade6-M210, ura4-D6,* Ch[16] [*ade6-M216*]) and YP10.22a (*h+*, *ade6-M210, ura4-D6,* Ch[16] (*ade6-M216*)), the isolation of the *mal3-1* carrying strain YP30.1 and the calculation of the minichromosome loss rate have been described (Fleig et al., 1996). Strains YP246 (*h−*, *his3-D1, leu1-32, ura4-D18, ade6-M210*) and YP249 (*h+*, *his3-D1, leu1-32, ura4-D18, ade6-M216*) (Ohi et al., 1996) were used to generate diploid strain YP41. The *mal3* deletion strain YP350 (*h+*, *mal3Δ::his3+, his3-D1, leu1-32, ura4-D18, ade6-M210*) was isolated by tetrad analysis. Strains YP113 (*h+*, *nda2-KM52, leu1-32*) and YP114 (*h+*, *nda3-KM311, leu1-32*) have been described (Umesono et al., 1983; Toda et al., 1984). Strains were grown in rich (YE5S) or EMM minimal medium with appropriate supplements (Moreno et al., 1991). For low- or high-level expression from the *nmt1+* promoter cells were grown in EMM with 15 μM thiamine or pregrown on EMM plus thiamine plates for 18 h at 30°C before inoculation into thiamine-less EMM liquid medium, respectively. Sensitivity to thiabendazole (TBZ) was monitored at 24 or 30°C on YE5S plates or EMM plates containing 10 μg/ml of TBZ.

Microscopy

Photomicrographs of cells were taken with a Zeiss Axioskop fitted with differential interference optics. For determination of phenotypes a minimum of 300 cells was scored microscopically. Staining with calcofluor (Sigma Chem. Co., St. Louis, MO) and processing of cells for immunofluorescence microscopy was carried out as described (Verde et al., 1995; Hagan and Hyams, 1988). For tubulin staining we used the primary monoclonal antitubulin antibody TAT1 (Woods et al., 1989) followed by FITC-conjugated goat anti–mouse antibodies (Hagan and Yanagada, 1997). Spindle pole bodies were stained using AP9.2 affinity-purified anti-sad1-primary and Cy3-conjugated secondary sheep anti–rabbit antibodies (Sigma) (Hagan and Yanagida, 1995). Immunofluorescence images were processed as described previously (Lange et al., 1995).

Identification of mal3+ ORF and Plasmid Constructions

Strain YP30.1 was transformed with an *S. pombe* genomic bank (Barbet et al., 1992) and Ura+ transformants were selected by incubation for 50 h at 32°C, followed by replica-plating twice onto plates containing 10 μg/ml TBZ. Plasmids were isolated (Moreno et al., 1991) from the 3 out of 24,000 transformants able to grow following this selection process, amplified in *E. coli* XL1-blue (Stratagene Inc., La Jolla, CA) and retransformed into YP30.1 to ascertain plasmid borne rescue. These plasmids were tested for the ability to suppress the increased minichromosome loss of the *mal3-1* mutant by visual screening for the suppression of colony sectoring. Only one of the genomic DNA inserts, present in pUR3-1, was able to rescue all defects of strain YP30.1.

30 nucleotides of sequence from the 5′ (5′TCGCTTATCTGTCCCT-TGAACCTACGACAA 3′) as well as the 3′ (5′GATCAGGTGGTA-ACTCAAAACCATCCTCAG 3′) end of the 2.9-kb genomic DNA insert of pUR3-1 were used for an homology search in the *S. pombe* database, identifying a region of identity on chromosome I that contained two putative ORFs SPAC18G6.13c and SPAC18G6.14. To determine which ORF rescued the *mal3-1* mutant strain, pUR3-1 was cut with PacI/SmaI and religated thus rendering pUR3-1a which contains only the SPAC-18G6.13c ORF. The 1.6 kb PvuI/BamHI fragment containing SPAC-18G6.14 was cloned blunt-ended into SmaI cut pUR18 (Barbet et al., 1992) resulting in plasmid pUR3-1b. Only pUR3-1b was able to rescue the defects of the *mal3-1* mutant. SPAC18G6.14 was thus named *mal3+*. To obtain full-length *mal3+*, genomic DNA prepared from strain YP10.22 (Moreno et al., 1991) was used as a PCR template with oligonucleotides *a* (5′TAC-CAGTCGAC*ATGTCTGAATCTCGGCAAGA* 3′) and *b* (5′CTTAGC-CCGGG*TTAAAACGTGATATTCTCATC* 3′). Oligonucleotides *a* and *b* are homologous to the 5′ and 3′ ends of the *mal3+* ORF (sequences in italics) and contain a SalI and SmaI site, respectively (see Fig. 1 *C*). These restrictions sites were used to clone the 980-bp *mal3+* PCR fragment into SalI/SmaI cut pREP3 (Maundrell, 1993) generating pREP3-mal3. The sequence of three independently PCR-derived *mal3+* DNAs was determined.

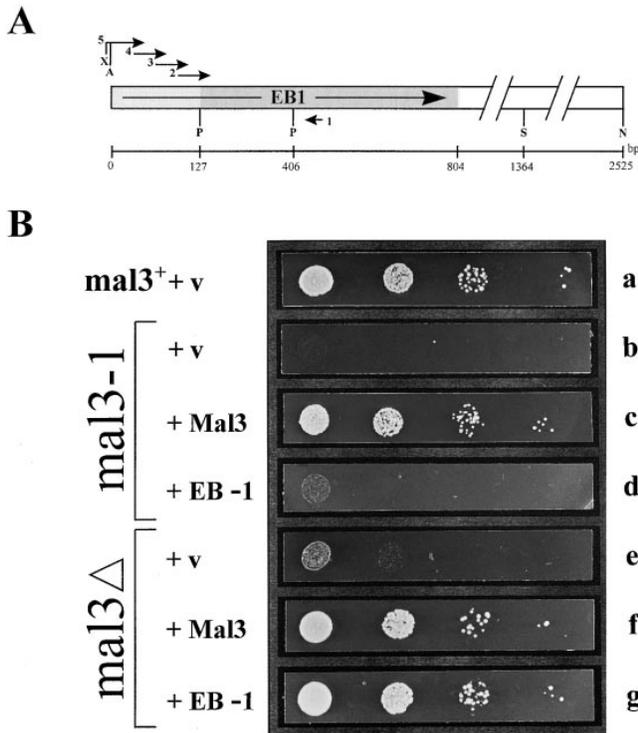To fuse the *yEGFP* and *mal3+* ORFs, we generated a *mal3+* ORF without the TAA stop codon via PCR using pREP3-mal3 and the following oligonucleotides: 5′TACCAGTCGACTATGTCTGAATCTCGCAAGA 3′ and 5′AGTACCTCGAGAAACGTGATATTCTCATCGT 3′ and cloned it into SalI/XhoI pBluescript (Stratagene). The *mal3+* DNA fragment was excised with BamHI/XhoI and cloned into BamHI/SalI cut pUG23 (Güldener, U., and J.H. Hegemann, unpublished observations), thereby fusing the *mal3+* and *yEGFP* (Cormack et al., 1997) ORFs. This fusion was subsequently cloned into SalI cut pREP3 behind the *nmt1+* promoter.

To demonstrate linkage between the cloned *mal3+* gene and the *mal3-1* mutant we constructed a *mal3Δ/mal3-1* diploid strain. Both *mal3* alleles show increased sensitivity to TBZ. Random spore analysis of this diploid strain revealed that the 400 spores tested showed increased sensitivity to TBZ indicating that *mal3Δ* and *mal3-1* were linked and thus that the complementing DNA fragment was the *mal3+* gene.

Database Searches and Cloning of Human EB-1

The NCBI's protein database was searched using BLASTP. The Mal3 query showed strongest homologies to human EB-1 (GenBank U24166; $P = 3.7 \times 10^{-53}$) and budding yeast protein Yer016p (GenBank P40013; $P = 4.3 \times 10^{-53}$). Sequence alignments were performed using CLUSTAL W (Thompson et al., 1994). The dbEST database was searched using BLAST. The EST clone (NCBI 184415, GenBank R13836) with the highest homology to Mal3 ($P = 1.8 \times 10^{-19}$) was ordered from Research Genetics Inc. (Huntsville, AL) (clone ID 26991) and sequenced revealing 100% identity to EB-1 (Su et al., 1995) albeit without the first 127 bp of the *EB-1* ORF. To obtain full-length *EB-1* the missing 5′ end of the

cDNA was constructed via PCR using the cDNA as template and overlapping oligonucleotides (see Fig. 2 A). Oligonucleotide 1 (5′ GCTGGAG-CAACAAGGGAA G 3′) was used in combination with oligonucleotides 2 (5′ AATCTGACAAAGATCGAACAGTTGTGCTCAGGGGCTGC-GTATTGTCAGTTTATGGAC 3′), 3 (5′ TGACATGCTGGCCTGGA-TCAATGAGTCTCTGCAGTTGAATCTGACAAAGATCGAACAG 3′), 4 (5′ TCAACGTCAGTGACCAGTGATAACCTAAGTCGACATGA-CATGCTGGCCTGGATC 3′), and 5 (5′ TTCTGCTCTAGACTCGA-GATGGCAGTGAACGTATACTCAACGTCAGTGACCAGTG 3′) in such a way that, for example, the PCR product resulting from the use of oligonucleotides 1 and 2 was used as a template for the next PCR (see Fig. 2 A). After sequence analysis of the 452-bp DNA product obtained from the last PCR reaction, the fragment was cloned as a PstI/XbaI fragment into pBluescript generating plasmid pJB17. To obtain the entire *EB-1* ORF the 2-kb long PstI/NotI fragment from the original cDNA clone was cloned into pJB17 resulting in plasmid pJB23. The 1,367-bp AvaI/StuI fragment from pJB23 containing the entire *EB-1* was cloned into XhoI/SmaI cut pREP3.

Disruption of mal3⁺ Open Reading Frame

To disrupt the *mal3⁺* gene we replaced the 0.8-kb PacI-PstI *mal3⁺* fragment with the 1.9-kb *his3⁺* (Ohi et al. 1996) marker in diploid strain YP41. Correct integration was verified by Southern-hybridization and PCR analysis. PCR primers used were: *a* (5′ GAGCCTCTTTGCGAAGGAG-CATTG 3′) and *b* (5′ TAAAACGTGATATTCTCATCGTCA 3′) homologous to the *his3⁺* 3′ end and the last 24 base pairs of the *mal3⁺* ORF, respectively. Transformants with a correctly disrupted *mal3⁺* ORF were sporulated and asci dissected by tetrad analysis.

Results

Isolation of the mal3-1 Mutant and Cloning of mal3⁺

Through a screen designed to isolate new fission yeast genes involved in chromosome segregation, we have identified 25 mutant strains which show an increase of loss rate of a nonessential minichromosome. A decrease in minichromosome transmission fidelity was identified by using an *ade6*-based colony color assay and was manifested as an increase in the number of red sectors in a white colony (Fleig et al., 1996). Strain YP30.1, which showed a 380-fold increase in minichromosome loss at 24°C (Fig. 1 A, *middle*) and was hypersensitive to the microtubule-destabilizing drug thiabendazole (TBZ) (Fig. 1 B), was chosen for further analysis. Crossing this mutant strain to a wild-type strain and pulling tetrads indicated that a single locus was responsible for both the increased loss of the minichromosome and the TBZ-sensitivity. We called this allele *mal3-1*.

The wild-type *mal3⁺* gene was isolated by complementation of the TBZ-sensitive phenotype. 10 μg/ml of TBZ had little effect on a *mal3⁺* strain at 30°C (Fig. 2 B, *a*), but severely inhibited growth of *mal3-1* (Fig. 1 B). Transformation of the *mal3-1* strain with an *S. pombe* genomic library identified three plasmids which were able to rescue the growth defect of the *mal3-1* strain on TBZ medium. One of these plasmids contained a 2.9-kb genomic DNA insert which also complemented the increased loss of the minichromosome (Fig. 1 A, *right*).

DNA sequence analysis of either end of this 2.9-kb insert was used for a homology search in the *Schizosaccharomyces pombe* database (Sanger Center, Hinxton, UK). A match of 100% identity was found on chromosome I. This region contained the two putative open reading frames (ORF) SPAC18G6.13c and SPAC18G6.14. The DNA insert contained the entire SPAC18G.13c ORF and 82% of the SPAC18G6.14 ORF (Fig. 1 C, *top diagram*). Only SPAC-

Figure 1. Phenotypic characterization of the *mal3-1* strain, isolation of *mal3⁺* gene and Mal3 amino acid sequence. (*A*) Sectoring phenotypes of *mal3⁺*, *mal3-1*, and *mal3-1* transformed with plasmid pUR3-1 strains grown at 24°C are shown. *Minichromosome loss rate; n. d., not determined. (*B*) While the *mal3-1* strain or *mal3-1* plus vector (pUR18) are unable to grow on TBZ containing EMM medium at 30°C, this defect is rescued by plasmid pUR3-1. (*C*) Diagrammatic representation of genomic DNA insert of pUR3-1 (*top*) and full length *mal3⁺* gene obtained by PCR (*bottom*). PCR primers have been marked by arrows, ORF by grey boxes and a putative intron in SPAC18G6.14/*mal3⁺* by a striped box. *P*, PvuI; *Pa*, PacI; *Ps*, PstI; *B*, BamHI; *Sm*, SmaI; *Sa*, SalI. (*D*) Amino acid sequence comparison of fission yeast Mal3, budding yeast Yer016p (GenBank accession number P40013) and human EB-1 (GenBank accession number U24166). Identical and similar amino acids are indicated by black and grey boxes, respectively. The arrow head indicates the end of the Mal3 truncated protein in pUR3-1. The *mal3⁺* sequence data are available from EMBL/GenBank/DDBJ under accession number Y09518.

18G6.14 rescued the *mal3-1* defects (data not shown) and was thus named *mal3⁺*. Linkage was demonstrated between the cloned *mal3⁺* gene and the *mal3-1* mutant (see Materials and Methods).

The DNA sequence of the *mal3⁺* ORF was identical to that reported for SPAC18G6.14 with the exception of a silent change at position 210 of the ORF where the *mal3⁺*

A

B

Figure 2. Suppression of the TBZ sensitivity of the *mal3-1* and *mal3Δ* strains by *mal3*[+] and *EB-1*. (*A*) Diagrammatic representation of cloning of *EB-1* cDNA. The positions of the five oligonucleotides used to construct the 5′ end (*lightly shaded box*) of *EB-1* not present in the original cDNA (*dark shaded box*) are indicated. *X*, XbaI; *A*, AvaI; *P*, PstI; *S*, StuI; *N*, NotI. (*B*) The *mal3*[+] strain transformed with vector (*a*), the *mal3-1* strain transformed with vector (*b*) or with plasmids expressing *mal3*[+](*c*) or *EB-1* (*d*) and the *mal3Δ* strain transformed with vector (*e*), or with plasmids expressing *mal3*[+] (*f*) or *EB-1* (*g*) were all grown for 18 h at 30°C in thiamine-less EMM medium, diluted in water and serial dilutions (1:10) starting with 10^4 cells were spotted on selective EMM medium with 10 μg/ml TBZ and incubated for 3 d at 30°C.

sequence had a C and SPAC18G6.14 a T nucleotide. *mal3*[+] encodes a protein of 308 amino acid residues with a mass of 35.1 kD and is interrupted by a 60-bp intron (Fig. 1, *C* and *D*). Database searches indicated that no previously characterized sequence motifs were present in the Mal3 amino acid sequence.

Mal3 Belongs to an Evolutionary Conserved Protein Family

A search of NCBI's nonredundant protein database identified several proteins with significant homology to Mal3, in particular the 30-kD human protein EB-1 (28.9% identity and 39.6% similarity) and the 38.3-kD hypothetical *S. cerevisiae* ORF Yer016p (33.1% identity and 44.1% similarity) (Su et al., 1995; Dietrich et al., 1997). Blocks of homology were distributed over the entire length of the protein with the exception of the COOH-terminal end (Fig. 1 *D*). Searches of the dbEST database (Boguski et al., 1993) identified 16 ESTs of human and mouse origin with significant homology to Mal3, indicating that it is a member of a conserved multiprotein family. Therefore we sought to determine whether members of this family were func-

tionally homologous. The EST cDNA clone with the highest homology to the Mal3 sequence was sequenced revealing 100% identity to the published sequence of human EB-1 (Su et al., 1995). The first 127 bp of the *EB-1* ORF not present in the cDNA fragment were generated via PCR using appropriate overlapping oligonucleotides (Fig. 2 *A*).

Human EB-1 Rescues the TBZ-Hypersensitivity of the mal3 Deletion Strain

The functional interchangeability of Mal3 and EB-1 proteins was tested by assessing the ability of EB-1 to suppress the TBZ-hypersensitive phenotype of *mal3-1* and *mal3Δ* (*mal3*[+] null allele, see next section). Both strains were transformed with plasmids expressing either *mal3*[+] or *EB-1* under the control of the thiamine-repressible *nmt1*[+] promoter. The presence of 15 μM thiamine leads to low-level expression from this promoter, while the absence of thiamine leads to high-level expression after 12–14 h (Fleig and Nurse, 1991; Maundrell, 1993). Transformants were pregrown in medium lacking thiamine for 18 h at 30°C and then tested for the ability to grow on TBZ-containing plates. As shown in Fig. 2 *B* the wild-type *mal3*[+] strain transformed with vector only grows well on plates containing 10 μg/ml TBZ (Fig. 2 *B*, *a*), while the *mal3Δ* strain grows poorly (*e*) and *mal3-1* is unable to grow (*b*). Plasmid-borne expression of Mal3 suppresses the growth defect on TBZ plates of both the *mal3-1* and *mal3Δ* mutants (Fig. 2 *B*, *c* and *f*). Human EB-1 partially rescued the increased TBZ-sensitivity of *mal3-1* (Fig. 2 *B*, *d*) and fully suppressed the TBZ sensitivity of *mal3Δ* (Fig. 2 *B*, *g*) suggesting that, while the human EB-1 protein is only partially able to compete with the mutant form of the Mal3 protein in the *mal3-1* strain, EB-1 can substitute for the complete loss of the *mal3*[+] gene product. Low-level expression of Mal3 and EB-1 partially rescued the TBZ-sensitivity of the *mal3Δ* strain (data not shown).

Deletion of the mal3[+] Gene Is Viable but Leads to Altered Cell Morphology and Phenotypes Similar to those of the mal3-1 Mutant

A *mal3* null allele was constructed by replacing the first 152 amino acids of the *mal3*[+] ORF and promoter region with the *his3*[+] marker in the diploid strain YP41 (Fig. 3 *A*, *diagram*). Southern analysis identified the resultant *mal3* deletion (data not shown). Diploid transformants that carried the *mal3*[+] null allele (named *mal3Δ*) were sporulated and subjected to tetrad analysis. While all four spores in each tetrad were viable at 32°C histidine prototrophy segregated 2:2, indicating that *mal3*[+] is not essential for cell proliferation. PCR analysis of the histidine prototrophic spores confirmed the correct integration of the *mal3*[+] disruption cassette (Fig. 3 *A*).

Further analysis of the haploid *mal3Δ* strain revealed phenotypes similar to those of the *mal3-1* mutant strain i.e., increased sensitivity to TBZ (Fig. 2 *B*, *e*) and a decreased transmission fidelity of the minichromosome (data not shown). In addition while no difference in growth between a wild-type and a *mal3Δ* strain was observed at 30 or 24°C (Fig. 3 *C*, *left*; data not shown), deletion of the *mal3*[+] gene conferred cold sensitivity (Fig. 3 *C*, *bottom right*).

Absence of the *mal3*[+] gene product resulted in alter-

A

B

C

mal3+

mal3Δ

30° C   20° C

D
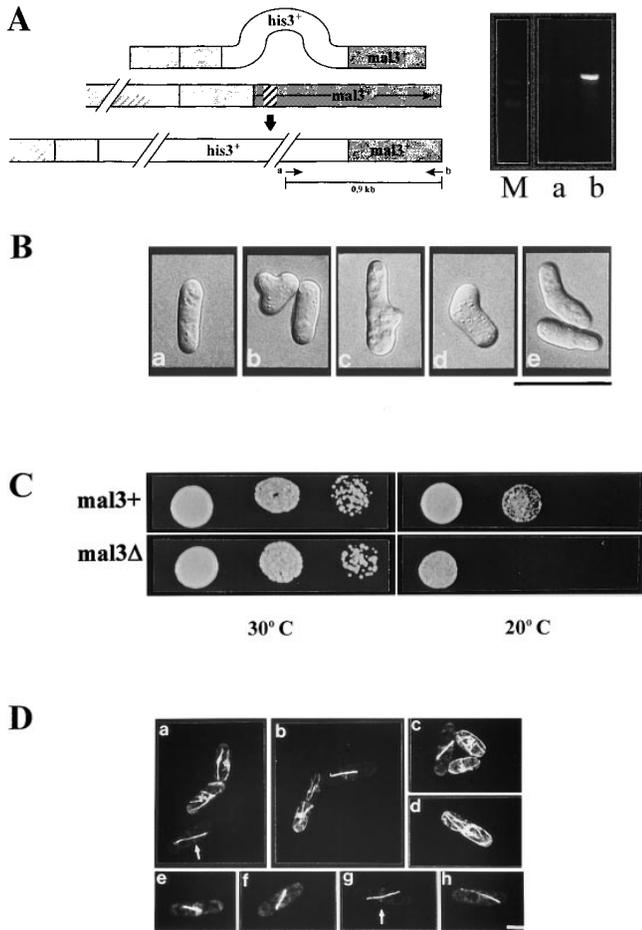
Figure 3. Phenotypic characterization of *mal3Δ* strain and in vivo localization of Mal3 protein. (*A*) Diagrammatic representation and PCR analysis of the *mal3+* disruption. Diploid strain YP41 was transformed with a linear 3.2-kb DNA fragment where 800 bp of the *mal3+* gene had been replaced by the 1.9-kb *his3+* gene. Spores were grown and their DNA analysed by PCR for the presence of the *mal3+* disruption. The positions of the PCR primers *a* and *b* are shown in the bottom diagram. The 900-bp DNA fragment generated by PCR can be obtained only if the linear *mal3+* disruption fragment has integrated correctly, as the DNA sequence homologous to primer *b* is not present on the 3.2-kb DNA fragment used for replacement. *a* and *b* show the PCR product of his⁻ and his⁺ spore DNA, respectively. *M*, DNA molecular mass markers (0.94 and 0.83 kb). (*B*) Photomicrographs of *mal3Δ* cells. A wild-type strain (*a*) and the *mal3Δ* strain (*b–e*) were grown logarithmically at 24°C. (*C*) Serial dilution patch test for cold-sensitivity of *mal3+* and *mal3Δ* strains. Dilutions shown were tenfold. Strains were incubated at 30°C and 20°C for 3 and 5 d, respectively. (*D*) In vivo localization of Mal3 protein. A wild-type *S. pombe* strain expressing Mal3-yEGFP under the control of the *nmt1+* promoter was pregrown on solid EMM thiamine medium, resuspended in liquid EMM medium with 0.05 μM thiamine, grown for 16 h at 30°C and photographed directly. Bars: (*B*) 20 μm; (*D*) 5 μm.

ations in cell form and polarity as branched and curved cells were seen instead of the cylindrical shape typical of wild-type cells (Figs. 3 *B* and 4 *A*). Bent cells were often elongated. Altered cell morphology was observed at all temperatures tested, but was most prominent at 20°C, where >30% of *mal3Δ* cells had abnormal shapes (Fig. 4 *A*).

A

mal3Δ (20°C)	17,4	15,5	18,3*	23,0‡
mal3Δ (32°C)	4,0	10,4	10,5	9,5
mal3+ (20°C)	0	< 1	< 2	< 1

B
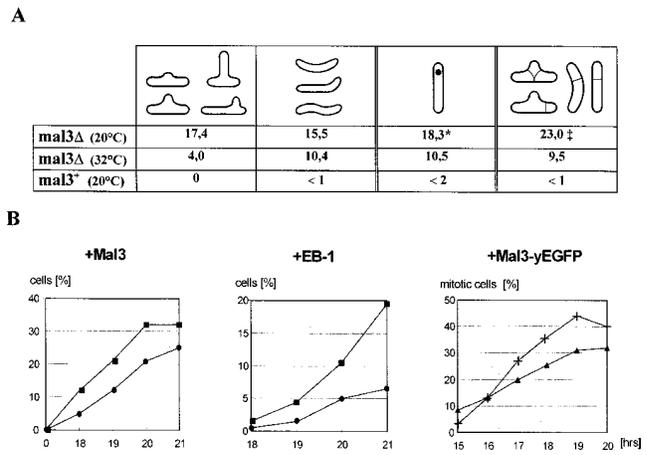
Figure 4. Phenotypes of the *mal3Δ* strain and Mal3 and EB-1 overproducing strains. (*A*) *mal3Δ* cells were grown at 20 or 32°C in liquid YE5S medium and the percentage of cells with abnormal cell morphology, a displaced nucleus and misplaced septum was determined. The *mal3+* control strain was grown at 20°C. *Percentage of all interphase cells with a displaced nucleus; ‡percentage of septated cells with a misplaced septum. (*B*) Wild-type strains overproducing Mal3, EB-1 or Mal3-yEGFP were grown for 0–21 h at 30°C in expression inducing medium and the percentage of cells with altered cell shape (●), a displaced nucleus (■), a mitotic spindle (▲) and aberrant spindles out of the total number of spindles (+) was determined.

The Mal3 Protein Associates with Microtubules In Vivo

To determine the intracellular localization of Mal3 in living cells, a yeast-enhanced version of the green fluorescent protein named yEGFP (Cormack et al., 1997) was fused to the COOH-terminal end of the *mal3+* coding region and the fusion protein was expressed under the control of the *nmt1+* promoter (see Materials and Methods). The Mal3-yEGFP fusion protein rescued the TBZ-sensitivity of *mal3Δ* when expressed at a high level from the *nmt1+* promoter, albeit less efficient than Mal3, indicating that the fusion protein was functional (data not shown).

We observed green fluorescence when the Mal3-yEGFP protein was expressed at low or high levels in the cell. Low-level expression of the fusion protein resulted in staining along microtubule structures and some uniform green fluorescence of the cytoplasm and faint nuclear staining. However, as fluorescence was weak under these conditions, we looked for intermediate levels of expression of the fusion protein which had no effect on cell growth and cell morphology but gave better staining. Growing cells on medium containing 0.05 μM thiamine (Javerzat et al., 1996; data not shown) resulted in fluorescence that was clearly highlighting filamentous structures reminiscent of microtubules. The Mal3-yEGFP fusion protein associated with both cytoplasmic (Fig. 3 *D*, *a–d*) and mitotic spindle microtubules (Fig. 3 *D*, *e–h*). Fluorescence was distributed uniformly along the elongating spindle, with early mitotic spindles staining most intensely. Interestingly in anaphase the Mal3-yEGFP fusion protein also localized to a ring present at the cell equator (Fig. 3 *D*, *a* and *g*, *arrows*). Expression of *yEGFP* alone from the *nmt1+* promoter led to uniform green staining of the entire yeast cell (data not shown; Fleig et al., 1996).

Loss of Mal3 Function Results in Altered Interphase Microtubule Arrays

As our data indicated that Mal3 is a microtubule interacting protein we examined the consequences of a loss of Mal3 protein upon the microtubule cytoskeleton.

In wild-type fission yeast cells cytoplasmic microtubules are aligned along the long axis of the cell between the cell tips (Marks et al., 1986; Hagan and Hyams, 1988; Fig. 5, *h* and *i*). In contrast morphologically wild-type *mal3Δ* cells grown at 20°C had microtubules that were largely short (approximately one-fifth of wild-type length) and present only around the nucleus (Fig. 5, *a* and *b*). In addition, the staining in branched cells was often absent or very weak possibly indicating that less than the wild-type complement of microtubules were present in each cytoplasmic bundle (data not shown). To determine that these findings were not artefacts of fixation, a simple test was performed. At the nonpermissive temperature *cdc25-22* cells arrest cell cycle progression at the G2/M boundary but continue to grow thus becoming highly elongated with cytoplasmic microtubules (Hagan and Hyams, 1988). By mixing arrested *cdc25-22* cells with shorter *mal3Δ* cells before processing them for immunofluorescence, one can determine whether the microtubules in both strains are unable to reach the cell tips (i.e., fixation artefact) or whether the defect is present only in *mal3Δ*. Consistent with the latter interpretation the images in Fig. 5 *k* show normal microtubules in the *cdc25-22* cell and short microtubules in *mal3Δ* cells. In contrast to the severe alteration of cytoplasmic microtubules no gross spindle abnormalities were observed in *mal3Δ* cells although again spindle staining was reduced. (Fig. 5 *k, arrowhead*). However we observed a fourfold increase in the number of cells showing condensed chromosomes in comparison to an isogenic wild-type strain indicating defects in some aspects of mitosis.

Consistent with the notion that the microtubule cytoskeleton plays a role in nuclear positioning (Toda et al., 1984; Hagan and Yanagida, 1997) *mal3Δ* cells frequently show displaced nuclei (Fig. 5 *l, small arrow*). At 20°C 18% of *mal3Δ* cells had off center premitotic nuclei (Fig. 4 *A*). Interestingly we also observed displaced post-anaphase-arrays (Fig. 5 *f*). Intriguingly the post-anaphase-arrays
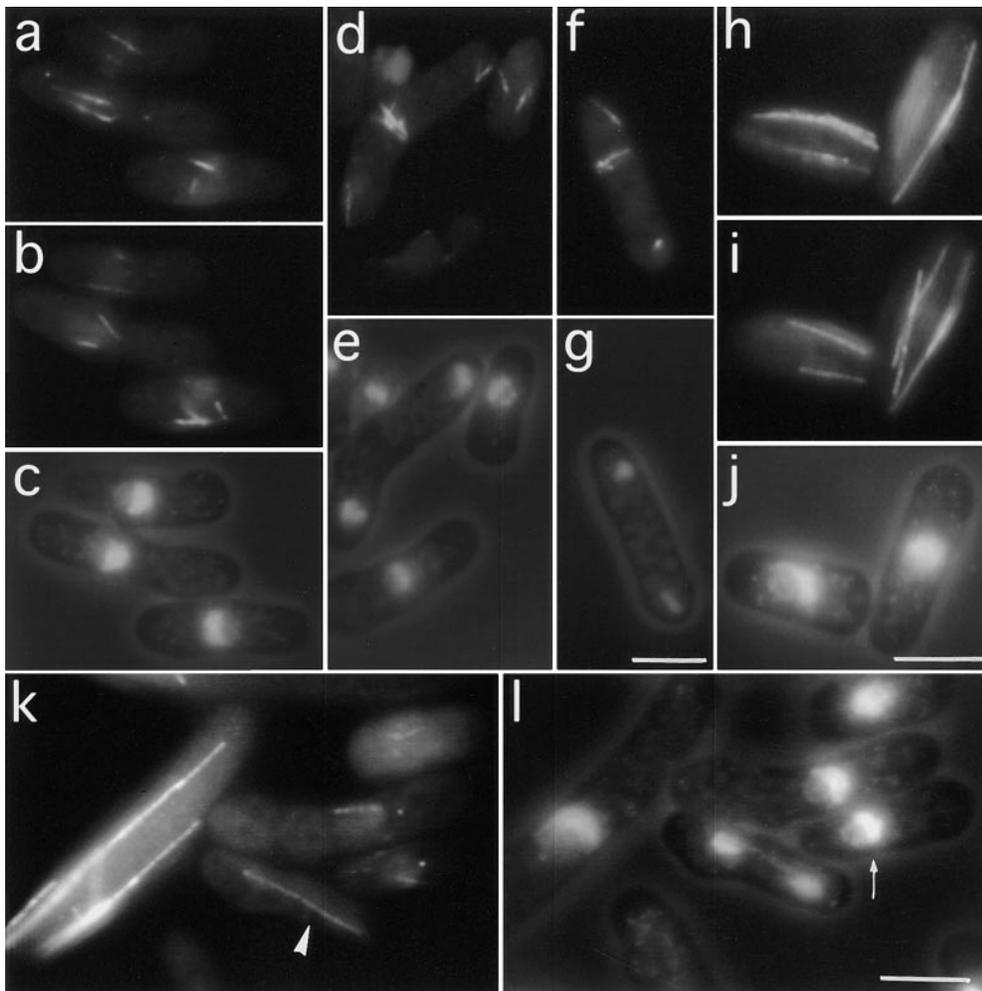
Figure 5. Antitubulin immunofluorescence images of *mal3Δ* cells cultured at 20°C. *a, b, d, f, h, i,* and *k* show antitubulin staining while *c, e, g, j,* and *l* show DAPI and phase contrast images. *a* and *b* represent two different focal planes of three *mal3Δ* cells showing several short microtubules around the location of the nucleus shown in *c.* (*d*) Strong post-anaphase-array staining in the upper, bent cell. (*f*) Displaced post-anaphase-array. *h–i* show antitubulin immunofluorescence images of two *mal3+* cells grown at 20°C at different focal planes, while *j* shows DAPI staining. *k* and *l* show a mixed culture of *mal3Δ* and elongated *cdc25-22* cells. *k* shows antitubulin while *l* shows DAPI staining. *cdc25-22* cells were grown at 25°C in YE5S to early log phase, shifted to the restrictive temperature for 210 min, returned to 20°C in 30 s by immersion in an ice bath and mixed at a ratio of 1:4 with the *mal3Δ* culture grown at 20°C inYE5S. *k* shows four *mal3Δ* cells and an elongated *cdc25-22* cell. The abnormally faint spindle in the *mal3Δ* cell is indicated by an arrow head in *k*. The small arrow in *l* indicates a *mal3Δ* cell with a misplaced nucleus. Bars, 5 μm.

were the most strongly staining structures in *mal3Δ* cells observed by antitubulin immunofluorescence possibly indicating that these microtubules have a different composition or properties to other cytoplasmic microtubules (Fig. 5 *d*).

In addition to displacement of the nucleus and post-anaphase-array lack of Mal3 also led to displacement of the septum from its normal central location. Approximately 23% of *mal3Δ* cells had a septum not positioned in the central fifth of a cell at 20°C (Fig. 4 *A*).

Overexpression of *mal3+* Inhibits Colony Formation and Leads to Aberrant Cell Morphology

Overproducing Mal3 by inducing *mal3+* expression from the *nmt1+* promoter in a wild-type strain resulted in severe inhibition of colony formation (Fig. 6 *A*, *b*) and cell elongation, indicative of a possible role of Mal3 in cell cycle regulation. Cells started to elongate following 18 h of induction and subsequently became highly elongated with phenotypes similar to those of the *mal3Δ* strain, i.e., aberrant cell morphologies and displaced interphase nuclei (Figs. 4 *B* and 6 *B*). The proportion of cells with altered cell shapes correlated directly with the duration of *mal3+* overexpression; the most drastic phenotypes were observed after 21 h or more (Figs. 4 *B* and 6 *C*, *b*).

Cells with extra Mal3 protein also displayed mitotic defects and were unable to undergo proper cytokinesis. The cytokinesis retardation appeared to be coupled with the appearance of abnormally formed and misplaced septa. Following 21 h of *mal3+* induction 7.2% of cells had a septum and in 25% of these the septa were not in the central fifth of the cell. Later (e.g., 24 h) more than 80% of cells with a septum showed highly abnormal, multiple and/or misplaced septa (Fig. 6 *C*, *d* and *f*). Overexpression of human EB-1 protein led to similar, albeit less severe phenotypes (Figs. 4 *B* and 6 *A*, *c* and *B*). Overexpression of either Mal3 or EB-1 protein in the *mal3Δ* strain led to moderate or no inhibition of colony formation, respectively (data not shown).

Overexpression of Mal3 Protein Compromises Spindle Formation and Function

Immunofluorescence staining of a wild-type strain overexpressing *mal3+* for 20–22 h at 32°C showed no gross defects in microtubule integrity in interphase cells. Cytoplasmic microtubule bundles were present in a full complement and extended along the main cell axis to the cell tips. The bundles in branched cells were slightly more curved than those of wild-type cells (Fig. 7 *e*).

Excess Mal3 led to an increase in the proportion of cells which were in mitosis and strongly affected the formation and function of the spindle. After 20 h of induction 24% of cells were in mitosis and 16% had condensed chromosomes. Two predominant defective spindle phenotypes were observed: (*a*) elongating spindles with severe defects in chromosome segregation to the poles (Fig. 7 *a*), and (*b*) the disintegration of the spindle evidenced by spindle fraying (Fig. 7, *a* and *b*) and two separated V-shaped tubulin structures present in one cell (Fig. 7, *d* and *g*). 52% of cells with a spindle exhibited the former phenotype, while 6% of all cells displayed the latter one. Additionally, 2.5% of cells in the population were unable to form a spindle and
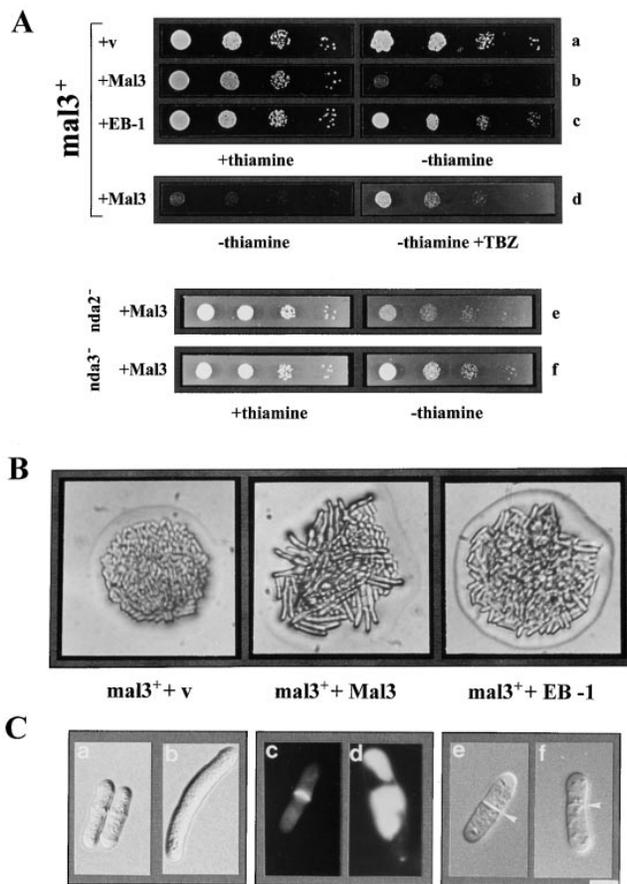
Figure 6. Phenotypic characterization of overexpression of Mal3 and EB-1 proteins. (*A*) Serial dilution patch test for inhibition of colony formation by overproduction of Mal3 and EB-1. Dilutions shown were tenfold. A *mal3+* strain was transformed with either the insert-less vector (*a*) or plasmids expressing *mal3+* (*b*) or *EB-1* (*c*) from the *nmt1+* promoter. Strains were grown for 18 h at 30°C in thiamineless medium and then plated on EMM medium with (+) or without thiamine (−).The growth inhibition phenotype of Mal3 overexpression was suppressed by 10 μg/ml TBZ (*d*) or the presence of the α- and β-tubulin mutants, *nda2-KM52* and *nda3-KM311*, respectively (*e* and *f*). Colonies were photographed after incubation for 3 d at 30 or 29°C (mutant tubulin strains). (*B*) Photomicrographs of colonies of wild-type cells transformed with vector control (*v*), or plasmids expressing *mal3+* or *EB-1*. Strains were pregrown as in *A* before streaking cells on thiamineless plates and incubating them for 1.5 d at 30°C. (*C*) *mal3+* was overexpressed in a wild-type strain for 0 (*a*, *c*, and *e*), 19 (*f*), 21 (*b*), or 24 (*d*) h at 30°C. *c* and *d* show staining of septa by calcofluor. Septa in *e* and *f* are indicated by arrowheads. Bar, 5 μm.

showed V-shaped tubulin staining patterns typical of mutants with a defective spindle pole body component or mitotic motor protein (Fig. 7, *c* and *f*; Hagan and Yanagida, 1995). We interpret the significant number of cells which showed two separate V-shaped structures in one cell as being those in which the two halves of the mitotic spindle no longer interdigitate and yet the microtubules are stable and do not depolymerize.

A time course analysis of Mal3-yEGFP overexpression revealed that the increase in the number of cells in mitosis and the appearance of aberrant spindle structures was cor-
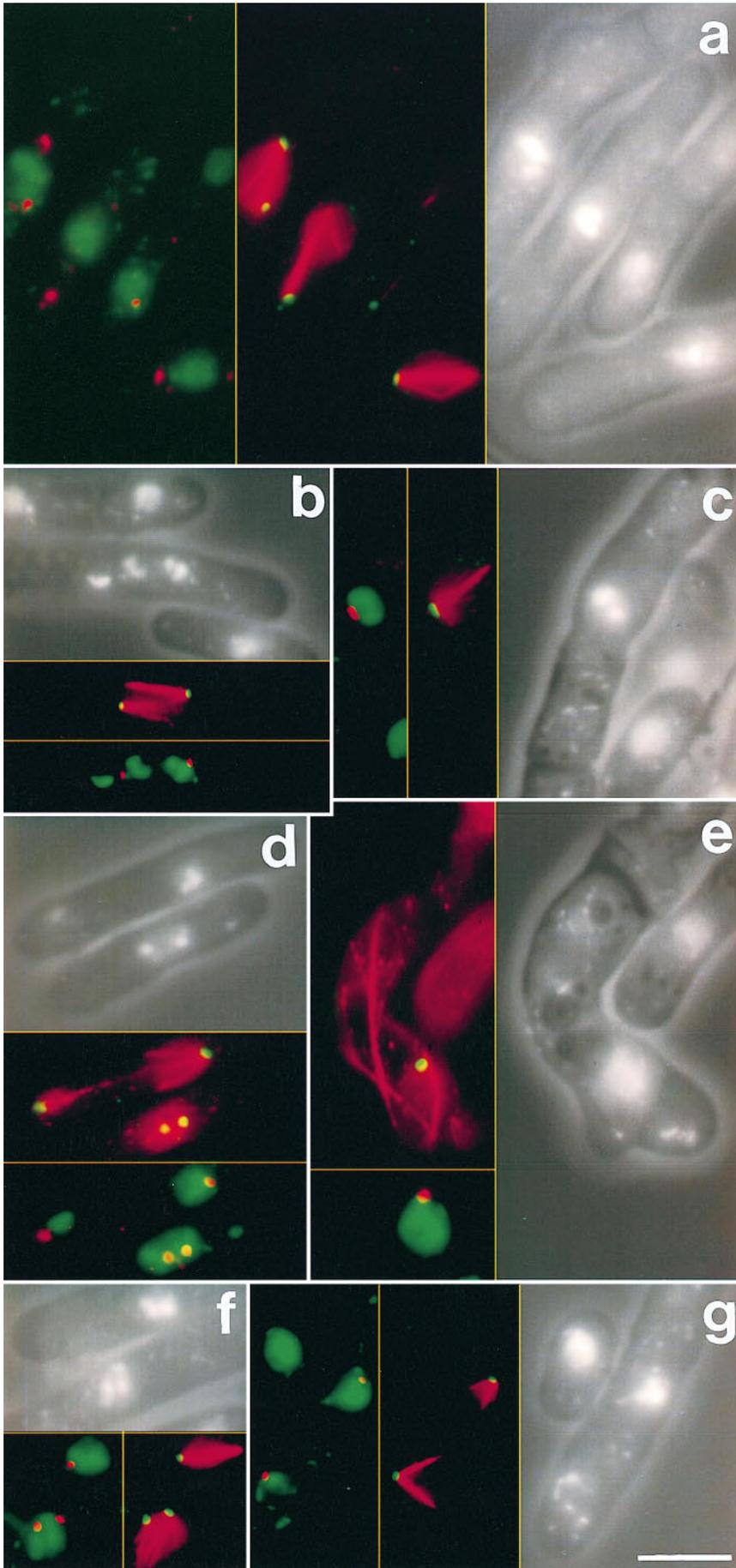
Figure 7. Overexpression of *mal3⁺* results in defects in form and function of the mitotic spindle. Wild-type cells overexpressing *mal3⁺* were grown at 32°C for 21 h in inducing conditions. Each panel shows three different images of the same cells: in the first, containing the lettering, the relative location of the chromatin and the cell outline is shown by combining DAPI fluorescence and phase contrast images; in the second the microtubules (*red*) and the SPBs (*green*) are shown; the third panel shows the position of the SPBs (*red*) relative to the chromatin (*green*). *a* shows three strongly staining spindles of roughly equal length. The chromosomes are highly condensed and randomly positioned along the spindle axis. In each case bars of tubulin staining emanate from the SPB away from the main body of the spindle. *b*, *d*, and *g* show examples of cells where the two half spindles appear to be losing their interdigitation presumably leading to the complete loss of interdigitation seen in *g*. In *b* the smaller chromosome III has wandered from the spindle axis, indicating that the microtubules are not contacting the kinetochores. *e* shows a bent interphase cell which has not separated from its partner during the previous cytokinesis. *c* and *f* show examples of defects during the early stages of spindle formation. Bar, 5 μm.

related directly with the duration of overexpression (Fig. 4 *B*, *right*) and peaked following induction for 19–20 h. At this time ~32% of cells showed green fluorescing mitotic spindles with >40% of these being aberrant.

Decreasing Microtubule Stability Partially Rescues the Mal3 Overexpression Phenotype of Severe Growth Inhibition

The abnormally short cytoplasmic microtubule arrays in the *mal3Δ* strain suggested that Mal3 might somehow influence microtubule stability. As excess Mal3 led to defective spindles and mitotic microtubules have shorter half-lives than their interphase counterparts (Salmon et al., 1984; Saxton et al., 1984) these data also support a possible role for Mal3 in stabilizing microtubules. If Mal3 does indeed play a role in stabilizing microtubules then destabilizing microtubules by some means would be expected to alleviate the severity of the phenotypes observed upon Mal3 overexpression. We tested this idea by destabilizing microtubules in two ways and assaying colony forming potential: first, wild-type cells overexpressing Mal3 were grown in the presence of TBZ and secondly by overproducing Mal3 in strains carrying the cold-sensitive mutant α1- and β-tubulin alleles, *nda2-KM52* and *nda3-KM-311*, respectively (Umesono et al., 1983). The inhibition of colony formation of wild-type cells expressing Mal3 at high levels was partially suppressed by growth on medium containing 10 μg/ml TBZ (Fig. 6 *A*, *d*) and was also rescued by the presence of either mutant tubulin allele (Fig. 6 *A*, *e–f*). The experiment was carried out at 29°C, which while being permissive for both mutant tubulin strains does result in 10–20% of cells having abnormal bent cell shapes (Umesono et al., 1983), indicating that the tubulin alleles do not impart a fully wild-type function. We tested three different transformants expressing extra Mal3 per strain and consistently found that while the presence of the *nda3-KM311* allele almost totally suppressed the inhibition of colony formation conferred by *mal3*[+] overexpression, the *nda2-KM52* allele was only partially able to do so.

Discussion

By a screen designed to isolate new components of the chromosome transmission machinery in fission yeast we have identified and characterized the *mal3*[+] gene. The *mal3-1* mutant strain shows a ~400-fold increase in the rate of loss of a nonessential minichromosome at 24°C but otherwise grows normally. However, as an increase in chromosome loss rate less than three orders of magnitude might not severely affect colony formation, we cannot rule out an effect of *mal3-1* on the transmission of regular chromosomes. Fission yeast Mal3 and the human APC-interacting protein EB-1 belong to the same protein family. Mutations in the APC gene result in the cancer predisposition syndrome FAP and are believed to be an early event in the development of the majority of sporadic colorectal tumors (reviewed in Kinzler and Vogelstein, 1996). Recently it has been demonstrated that the genetic instability that forms an integral part of colorectal tumors can be caused by severe defects in chromosome segregation (Lengauer et al., 1997). In this context it is intriguing that we have identified

the *mal3*[+] gene product, whose loss can be rescued by human EB-1, in a screen for components influencing chromosome transmission fidelity in fission yeast.

Mal3 Is a Microtubule-associated Protein that Influences Microtubule Integrity

In vivo localization of the Mal3 fusion protein showed, in addition to faint cytoplasmic and nuclear staining, strong fluorescence associated with both cytoplasmic and mitotic microtubules (Fig. 3 *D*). As is the case with antitubulin immunofluorescence mitotic spindles were brighter than cytoplasmic microtubules, consistent with more microtubules in spindles as opposed to the cytoplasmic microtubule bundles (Ding et al., 1993). These data strongly indicate that Mal3 interacts with microtubules although we do not yet know if the interaction is a direct one.

Indirect antitubulin immunofluorescence of *mal3Δ* cells showed altered microtubule structures. Instead of the typical wild-type cytoplasmic microtubule network that extends between the cell tips (Hagan and Hyams, 1988; Fig. 5, *h* and *i*) the interphase microtubules of the *mal3Δ* strain were extremely short, never reached the cell tips and were closely associated with the nucleus (Fig. 5, *a* and *b*). Regrowth of microtubules after depolymerization by incubation at low temperatures shows microtubule regrowth occurs predominantly around the nucleus (cited in Verde et al., 1995; Hagan, I.M., unpublished observations). The often fainter staining of microtubules in the *mal3*[+] deletion strain indicates either poor fixation or fewer microtubules as opposed to the bundles of three microtubules observed in wild-type *S. pombe* cells (Streiblova and Girbardt, 1980; Tanaka and Kanbe, 1986).

The effect on spindle morphology was less marked in *mal3Δ* cells with the only visible defect being weaker staining intensity (Fig. 5, *k*). However a *mal3Δ* cell population showed a significantly increased chromosome condensation index indicating a delay during mitosis suggesting that the weaker staining reflects a compromised function. This finding is complemented by the observation that deletion of the *mal3*[+] homologue in *S. cerevisiae* leads to an accumulation of cells with a 2C DNA content (Fleig, U., S. Heck, and J.H. Hegemann, unpublished observation).

Overproduction of the Mal3 protein severely compromised the formation and function of the mitotic spindle. Microtubules can be altered by the association of microtubule associating proteins (MAP) and interaction with microtubule severing proteins and motors (reviewed in Hirokawa, 1994; Desai and Mitchison, 1995; Hyman and Karsenti, 1996). Mitotic microtubules have shorter half-lives than interphase microtubules and microtubule turnover plays an important part in the assembly of the mitotic spindle (reviewed in Hyman and Karsenti, 1996). In addition proteins that increase the catastrophe rate of microtubules are required for correct mitotic spindle assembly (Belmont and Mitchison, 1996; Walczak et al., 1996). We speculate that overexpression of Mal3 might hyperstabilize microtubules and thus upset the fine-tuned balance of microtubule dynamics required for mitosis. In this context it is interesting that the *mal3*[+] overexpression phenotype of severe growth inhibition was rescued partially by growth on TBZ-containing medium or in the presence of mutant

tubulin alleles (Fig. 6 *A, d–f*). Rescue of a number of phenotypes caused by the absence of the microtubule-destabilizing mitotic motor protein Kar3p has also been observed in the presence of microtubule-destabilizing drugs or a reduction in tubulin gene dosage (Saunders et al., 1997).

An alternative explanation for the effect of excess Mal3 on the mitotic spindle could be that the excess protein is coating the mitotic microtubules, thus blocking/hindering binding of proteins required for proper spindle function.

Absence or Overexpression of Mal3 Protein Results in Displacement of Nucleus and Septum

The interphase nucleus of *mal3Δ* cells was often displaced from the center of the cells (Fig. 4 *A*), thus reinforcing the role played by the microtubule cytoskeleton and associated motor proteins in the positioning of the nucleus (for example Oakley and Morris, 1980; Jacobs et al., 1988; Hagan and Yanagida, 1997). In *S. pombe*, mutations in tubulin genes or the presence of microtubule-destabilizing chemicals can lead to a displacement of the nucleus (Walker, 1982; Umesono et al., 1983; Hiraoka et al., 1984; Verde et al., 1995).

Excess Mal3 protein also had a profound effect on the morphology and position of the division septum, resulting in abnormal and/or misplaced septa (Fig. 6 *C, d* and *f*) reminiscent of loss of function mutations in the fission yeast *dmf1/mid1* gene, which is required for the correct positioning of the division septum (Chang et al., 1996; Sohrmann et al., 1996). A possible connection between the actin and microtubule cytoskeleton has been demonstrated in *S. pombe* by the existence of the benomyl-resistant *ben4* mutant, which displays an altered actin cytoskeleton and is rendered lethal by the presence of an extra actin gene in the genome (Fantes, 1989). In this context the existence of an equatorial tubulin ring present in anaphase after the formation of the actin contractile ring is particularly interesting and led to the suggestion that this microtubule ring also plays a role in the determination of the division plane (Pichova et al., 1995). Similarly rings have also been observed with the in vivo localization of the *S. pombe* microtubule-associating protein Dis1 (Nabeshima et al., 1995) and our Mal3-yEGFP.

Deletion or Overexpression of mal3+ Leads to Aberrant Cell Morphology

A large number of abnormal curved or branched cells were observed in the *mal3Δ* strain and in cells overexpressing *mal3+* indicating a possible role for Mal3 in the control of directed cell growth. The altered cell shape is most likely a consequence of the defective microtubule cytoskeleton of the *mal3Δ* strain as disruption or alteration of the microtubule cytoskeleton by mutation of the tubulin genes or by treatment with microtubule-destabilizing chemicals also leads to misshaped cells (Walker, 1982; Umesono et al., 1983; Hiraoka et al., 1984; Verde et al., 1995). The molecular basis for the importance of the microtubular cytoskeleton in the spatial organization of fission yeast has begun to emerge with the characterization of the *tea1+* gene product, whose localization at the cell poles is dependent upon an intact cytoplasmic microtubule cytoskeleton and which is required to maintain antipodal growth (Mata and Nurse, 1997).

Excess Mal3 also resulted in morphological abnormalities in the presence of seemingly normal interphase microtubule arrays. This resembles the effect of overexpression of the microtubule-interacting protein Dis1 (Nabeshima et al., 1995; Nakaseko et al., 1996). The most likely explanation for these phenotypes is that the overproduction of a MAP occupies so many binding sites on the microtubule surface that it either directly competes out or sterically blocks the binding of other MAPs and motors. Thus the microtubules appear normal but are nonfunctional.

Function of the Human APC-interacting Protein EB-1?

The tumor suppressor protein APC has been implicated in a number of cellular processes including cell migration (Kinzler and Vogelstein, 1996; reviewed in Pfeifer, 1996). Although mutations in APC lead to an accumulation of enterocytes close to the crypt-villus transition in the intestine (reviewed in Polakis, 1995), overexpression of wild-type APC protein results in disordered cell migration in the intestinal epithelium of chimeric mice (Wong et al., 1996). In the presence of an intact microtubule cytoskeleton, endogenous APC protein in epithelial cells is concentrated in puncta near the end of microtubules that protrude into actively migrating membrane structures (Näthke et al., 1996). As the APC protein can promote assembly and bundling of microtubules in vitro (Munemitsu et al., 1994), one of its functions might be the recruitment of microtubules to protruding membrane structures thereby stabilizing/determining the direction of cell migration (Näthke et al., 1996). The important role of microtubule dynamics in guiding directed movement of, for example, the motile portion of the axon terminal, the growth cone, has been well documented (Sabry et al., 1991; Tanaka and Kirschner, 1995).

The carboxyl terminus of APC is required for the association with both microtubules and EB-1 (Munemitsu et al., 1994; Smith et al., 1994; Su et al., 1995). As human EB-1 and fission yeast Mal3 appear to have similar functions and our data indicate that Mal3 is a microtubule-interacting protein involved in microtubule integrity, we suggest that APC might exert the recruitment of microtubules to actively migrating membranes via EB-1 protein. Whether EB-1 is normally distributed all over microtubules (as is the case for Mal3) and APC only interacts with a sub-population, or whether EB-1 is always complexed with APC and microtubule ends awaits further analysis. Indeed interaction with APC might be only one of multiple functions executed by EB-1.

The control of directed cell growth is vital for cell function and cellular differentiation. The cylindrical form of the wild-type fission yeast cell and the highly polarized manner of growth of this organism facilitate the identification of components required for these processes. Our results raise the exciting possibility that some of the components required for directed cell growth in fission yeast and directed cell movement in higher eucaryotes have been conserved.

References

Barbet, N., W.J. Muriel, and A.M. Carr. 1992. Versatile shuttle vectors and genomic libraries for use with *Schizosaccharomyces pombe. Gene (Amst.).* 114: 59–66.

Boguski, M.S., T.M.J. Lowe, and C.M. Tolstoshev. 1993. dbEST-database for "Expressed Sequence Tags." *Nat. Genet.* 4:332–333.

Belmont, L.D., and T.J. Mitchison. 1996. Identification of a protein that interacts with tubulin dimers and increases the catastrophe rate of microtubules. *Cell.* 84:623–631.

Chang F., A. Wollard, and P. Nurse. 1996. Isolation and characterization of fission yeast mutants defective in the assembly and placement of the contractile ring. *J. Cell. Sci.* 109:132–142.

Cormack, B.P.,G. Bertram, M. Egerton, N.A. Gow, S. Falkow, and A.J. Brown. 1997. Yeast-enhanced green fluorescent protein (yEGFP) a reporter of gene expression in Candida albicans. *Microbiology.* 143:303–311.

Desai, A., and T.J. Mitchison. 1995. A new role for motor proteins as couplers to depolymerizing microtubules. *J. Cell Biol.* 128:1–4.

Dietrich, F.S., J. Mulligan, K. Hennessy, M.A. Yelton, E. Allen, R. Araujo, E. Aviles, A. Berno, T. Brennan, J. Carpenter et al. 1997. The nucleotide sequence of Saccharomyces cerevisiae chromosome V. *Nature (Lond.).* 387(suppl):78–81.

Ding, R., K.L. McDonald, and J.R. McIntosh. 1993. Three-dimensional reconstruction and analysis of mitotic spindles from the yeast, *Schizosaccharomyces pombe. J. Cell Biol.* 120:141–151.

Fantes, P.A. 1989. Molecular biology of the fission yeast. Academic Press, San Diego. 127–182.

Fleig, U.N., and P. Nurse. 1991. Expression of a dominant negative allele of *cdc2* prevents activation of the endogenous p34[cdc2] kinase. *Mol. Gen. Genet.* 226:432–440.

Fleig, U., M. Sen-Gupta, and J.H. Hegemann. 1996. Fission yeast *mal2*[+] is required for chromosome segregation. *Mol. Cell Biol.* 16:6169–6177.

Groden, J., A. Thliveris, W. Samowitz, M. Carlson, L. Gelbert, H. Albertsen, G. Joslyn, J. Stevens, L. Spirio, M. Robertson et al. 1991. Identification and characterization of the familial adenomatous polyposis coli gene. *Cell.* 66: 589–600.

Hagan, I.M., and J.S. Hyams. 1988. The use of cell division cycle mutants to investigate the control of microtubule distribution in the fission yeast *Schizosaccharomyces pombe. J. Cell Sci.* 89:343–357.

Hagan, I., and M. Yanagida. 1995. The product of the spindle formation gene *sad1*[+] associates with the fission yeast spindle pole body and is essential for viability. *J. Cell Biol.* 129:1033–1047.

Hagan, I., and M. Yanagida. 1997. Evidence for cell cycle-specific, spindle pole body mediated nuclear positioning in the fission yeast *Schizosaccharomyces pombe. J. Cell Sci.* 110:1851–1866.

Hartwell, L. 1992. Defects in a cell cycle checkpoint may be responsible for the genomic instability of cancer cells. *Cell.* 71:543–546.

Hiraoka, Y., T. Toda, and M. Yanagida. 1984. The *nda3* gene of fission yeast encodes β-tubulin: a cold sensitive *nda*3 mutation reversibly blocks spindle formation and chromosome movement in mitosis. *Cell.* 39:349–358.

Hirokawa, N. 1994. Mikrotubule organization and dynamics dependent on microtubule-associated proteins. *Curr. Opin. Cell Biol.* 6:74–81.

Hoyt, M.A., and J.R. Geiser. 1996. Genetic analysis of the mitotic spindle. *Annu. Rev. Genet.* 30:7–33.

Hyman, A.A., and E. Karsenti. 1996. Morphogenetic properties of microtubules and mitotic spindle assembly. *Cell.* 84:401–410.

Jacobs, C.W., A.E.M. Adams., P.J. Szaniszlo, and J.R. Pringle. 1988. Functions of microtubles in the *Saccharomyces cerevisiae* cell cycle. *J. Cell Biol.* 107: 1409–1426.

Javerzat, J.-P., G. Cranston, and R.C. Allshire. 1996. Fission yeast genes which disrupt mitotic chromosome segregation when overexpressed. *Nucleic Acids Res.* 24:4674–4683.

Kemler, R. 1993. From cadherins to catenins: cytoplasmic protein interactions and regulation of the cell adhesion. *Trends Genet.* 9:317–321.

Kinzler, K.W., and B. Vogelstein. 1996. Lessons from hereditary colorectal cancer. *Cell.* 87:159–170.

Lange, B.H., T. Sherwin, I.M. Hagan, and K. Gull. 1995. The basics of immunofluorescence video-microscopy for mammalian cells and microbial systems. *Trends in Cell Biol.* 5:328–332.

Lengauer, C., K.W. Kinzler, and B. Vogelstein. 1997. Genetic instability in colorectal cancers. *Nature (Lond.).* 386:623–627.

Marks, J., I.M. Hagan, and J.S. Hyams. 1986. Growth polarity and cytokinesis in fission yeast: the role of the cytoskeleton. *J. Cell. Sci.(Suppl.).* 5:229–241.

Mata, J., and P. Nurse. 1997. tea1 and the microtubular cytoskeleton are important for generating global spatial order within the fission yeast cell. *Cell.* 89: 939–949.

Matsumine, A., A. Ogai, T. Senda, N. Okumura, K. Satho, G.-H. Baeg, T. Kawahara, S. Kobayashi, M. Okada, K. Toyoshima, and T. Akiyama. 1996. Binding of APC to the human homolog of the drosophila discs large tumor suppressor protein. *Science (Wash. DC).* 272:1020–1023.

Maundrell, K.G. 1993. Thiamine repressible expression vectors pREP and pRIP for fission yeast. *Gene (Amst.).* 123:127–130.

Moreno, S., A. Klar, and P. Nurse. 1991. Molecular genetic analysis of fission yeast *Schizosaccharomyces pombe. Methods Enzymol.* 194:795–823.

Munemitsu S., B. Souza, O. Müller, I. Albert, B. Rubinfeld, and P. Polakis. 1994. The APC gene product associates with microtubules in vivo and promotes their assembly in vitro. *Cancer Res.* 54:3676–3681.

Nabeshima, K., H. Kurooka, M. Takeuchi, K. Kinoshita, Y. Nakaseko, and M. Yanagida. 1995. p93[dis1], which is required for sister chromatid separation, is a novel microtubule and spindle pole body-associating protein phosphorylated at the Cdc2 target sites. *Genes Dev.* 9:1572–1585.

Nakaseko, Y., K. Nabeshima, K. Kinoshita, and M. Yanagida. 1996. Dissection of fission yeast microtubule associating protein p93[Dis1]: regions implicated in regulated localization and microtubule interaction. *Genes to Cells.* 1:633–644.

Näthke, I.S., C.L. Adams, P. Polakis, J.H. Sellin, and W.J. Nelson. 1996. The adenomatous polyposis coli tumour suppressor protein localizes to plasma membrane sites involved in active cell migration. *J. Cell Biol.* 134:165–179.

Nishisho, I., Y. Nakamura, Y. Miyoshi, Y. Miki, H. Ando, A. Horii, K. Koyama, J. Utsonomiya, S. Baba, and P. Hedge. 1991. Mutation of chromosome 5q21genes in FAP and colorectal cancer patients. *Science (Wash. DC).* 253: 665–669.

Niwa, O., T. Matsumoto, and M. Yanagida. 1986. Construction of a mini-chromosome by deletion and its mitotic and meiotic behaviour in fission yeast. *Mol. Gen. Genet.* 203:397–405.

Oakley, B.R., and N.R. Morris. 1980. Nuclear movement is β-tubulin dependent in Aspergillus nidulans. *Cell.* 19:255–262.

Ohi, R., A. Feoktistova, and K.L. Gould. 1996. Construction of vectors and a genomic library for use with his3-deficient strains of *Schizosaccharomyces pombe. Gene (Amst.).* 174:315–318.

Pfeifer, M. 1996. Regulating cell proliferation: as easy as APC. *Science (Wash. DC).* 272:974–975.

Pichova, A., S.D. Kohlwein, and M. Yamamoto. 1995. New arrays of cytoplasmic microtubules in the fission yeast *Schizosaccharomyces pombe. Protoplasma.* 188:252–257.

Polakis, P. 1995. Mutations in the APC gene and their implications for protein structure and function. *Curr. Opin. Genet. Dev.* 5:66–71.

Sabry, J.H., T.P. O'Connor, L. Evans, A. Toroian-Raymond, M. Kirschner, and D. Bentley. 1991. Microtubule behavior during guidance of pioneer neuron growth cones in sito. *J. Cell Biol.* 115:381–395.

Salmon, E.D., R.J. Leslie, W.M. Karow, J.R. McIntosh, and W.M. Saxton. 1984. Spindle microtubule dynamics in sea urchin embryos: analysis using fluorescence-labeled tubulin and measurements of fluoresence distribution after photobleaching. *J. Cell Biol.* 99:2165–2186.

Saunders, W., D. Hornack, V. Lengyel, and C. Deng. 1997. Kar3p acts at preanaphase spindle poles to limit the number and length of cytoplasmic microtubules. *J. Cell Biol.* 137:417–431.

Saxton, W.M., D.L. Stemple, R.J. Leslie, E.D. Salmon, M. Zavortink, and J.R. McIntosh. 1984. Tubulin dynamics in cultured mammalian cells. *J. Cell Biol.* 99:2175–2186.

Sohrmann, M., C. Frankhauser, C. Brodbeck, and V. Simanis. 1996. The *dmf1/mid1* gene is essential for correct positioning of the division septum in fission yeast. *Genes Dev.* 10:2707–2719.

Smith, K.J., D.B. Levy, P. Maupin, T.D. Pollard, B. Vogelstein, and K.W. Kinzler. 1994. Wild-type but not mutant APC associates with the microtubule cytoskeleton. *Cancer Res.* 54:3627–3675.

Streiblova, E., and M. Girbardt. 1980. Microfilaments and microtubules in cell division cycle mutants of *Schizosaccharomyces pombe. Can. J. Microbiol.* 26: 250–261.

Su, L.-K., M. Burrell, D.E. Hill, J. Gyuris, R. Brent, R. Wiltshire, J. Trent, B. Vogelstein, and K.W. Kinzler. 1995. APC binds to the novel protein EB-1. *Cancer Res.* 55:2972–2977.

Tanaka, E., and M.W. Kirschner. 1995. The role of microtubule dynamics in growth cone motility and axonal elongation. *J. Cell Biol.* 128:139–155.

Tanaka, K., and T. Kanbe. 1986 Mitosis in the fission yeast *Schizosaccharomyces pombe* as revealed by freeze-substitution electron microscopy. *J. Cell Sci.* 80:253–268.

Thompson, J.D., D.G. Higgins, and T.J. Gibson. 1994. CLUSTAL W: improving the sensitivity of progressive multiple sequence alignment through sequence weighting, position-specific gap penalties and weight matrix choice. *Nucleic Acids Res.* 22:4673–4680.

Toda, T., Y. Adachi, Y. Hiraoka, and M. Yanagida. 1984. Identification of the pleiotropic cell division gene NDA2 as one of the two different α-tubulin genes in *Schizosaccharomyces pombe. Cell.* 37:233–242.

Umesono, K., T. Toda, S. Hayashi, and M. Yanagida. 1983. Two cell division cycle genes NDA2 and NDA3 of the fission yeast *Schizosaccharomyces pombe* control microtubular organization and sensitivity to anti-mitotic benzimida-

zole compounds. *J. Mol. Biol.* 168:271–284.

Verde, F., J. Mata, and P. Nurse. 1995. Fission yeast cell morphogenesis: identification of new genes and analysis of their role during the cell cycle. *J. Cell Biol.* 131:1529–1538.

Walker, G.M. 1982. Cell cycle specificity of certain anti-microtubular drugs in *Schizosaccharomyces pombe*. *J. Gen. Micro.* 128:61–71.

Walczak, C.E., T.J. Mitchison, and A. Desai. 1996. XKCM1: a Xenopus kinesin-related protein that regulates microtubule dynamics during mitotic spindle assembly. *Cell.* 84:37–47.

Walczak, C.E., and T.J. Mitchison. 1996. Kinesin-related proteins at mitotic spindle poles. Function and regulation. *Cell.* 85:943–946.

Wong, M.H., M.L. Hermiston, A.J. Syder, and J.I. Gordon. 1996. Forced expression of the tumour suppressor adenomatosis polyposis protein induces disordered cell migration in the intestinal epithelium. *Proc. Natl. Acad. Sci. USA.* 93:9588–9593.

Woods, A., T. Sherwin, R. Sassa, T.H. MacRae, A.J. Baines, and K. Gull. 1989. Definition of individual components within the cytoskeleton of *Trypanosoma brucei* by a library of monoclonal anitbodies. *J. Cell Sci.* 93:491–500.

Yanagida, M. 1995. Frontier questions about sister chromatid separation in anaphase. *Bioessays.* 17:519–526.